

# Scalar PWM Implementation Methods for Three-phase Three-wire Inverters

N. Onur Çetin, Ahmet M. Hava

Department of Electrical and Electronics Engineering, Middle East Technical University, Ankara, TURKEY  
ocetin@eee.metu.edu.tr, hava@metu.edu.tr

## Abstract

There are various PWM methods proposed for three-phase voltage source inverters. Each method has unique performance characteristics (voltage linearity, ripple voltage/current, common mode voltage/current, switching loss, etc.). Scalar and vector implementation are two main techniques for implementation of PWM methods. Scalar techniques provide equivalent performance to vector implementation and are more favorable for implementation due to simplicity. This paper proposes simple scalar implementation techniques for the popular high performance PWM methods. In the paper the practical implementation of various PWM methods is discussed and the laboratory experiments are shown.

## 1. Introduction

Three-phase three-wire voltage-source inverters (VSI) are widely utilized in ac motor drive, utility interface applications with high performance and high efficiency. In Fig. 1, a standard three-phase two-level VSI circuit diagram is illustrated. The classical VSIs generate AC output voltage from DC input voltage with required magnitude and frequency by programming high-frequency rectangular voltage pulses. The carrier-based pulse width modulation (PWM) is the preferred approach in most applications due to the low-harmonic distortion waveform characteristics with well-defined harmonic spectrum, the fixed switching frequency, and implementation simplicity.

Carrier-based PWM methods employ the “per-carrier cycle volt-second balance” principle to program a desirable inverter output voltage waveform [1]. There are two main implementation techniques: scalar implementation and space vector implementation. In the scalar approach, as shown in Fig. 2, a modulation wave is compared with a triangular carrier wave and the intersections define the switching instants. In the space vector approach, as illustrated in the space vector diagram in Fig. 3, the time length of the inverter states are pre-calculated for each carrier cycle by employing space vector theory and the voltage pulses are directly programmed [1].

There are various PWM methods which can be implemented via scalar or vector method. These methods differ in terms of their voltage linearity range, ripple voltage/current, switching losses, and high frequency common mode voltage/current properties. Conventional sinusoidal PWM (SPWM), space vector PWM (SVPWM) [1], discontinuous PWM1 (DPWM1) [1], active zero state PWM (AZSPWM) methods [2], near state PWM (NSPWM) [3], and remote state PWM (RSPWM) methods [4], are a few to name.

This paper reviews the PWM principles, the popular PWM methods, and provides simple scalar PWM implementation method (for most methods) which is favorable over the space

vector PWM implementation. The experimental results verify the feasibility of the proposed approach.

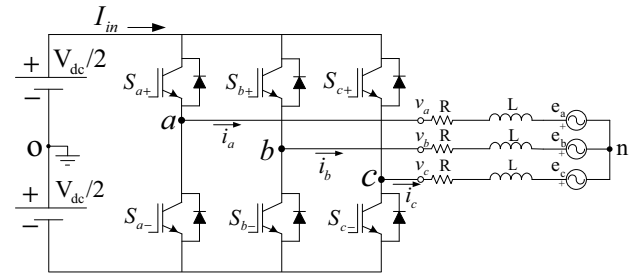


Fig. 1. Circuit diagram of a PWM-VSI drive connected to an R-L-E type load.

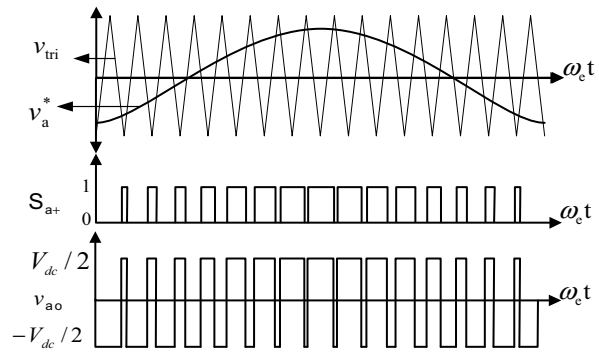


Fig. 2. Triangle intersection PWM phase “a” modulation wave, switching signal and  $v_{ao}$  voltage.

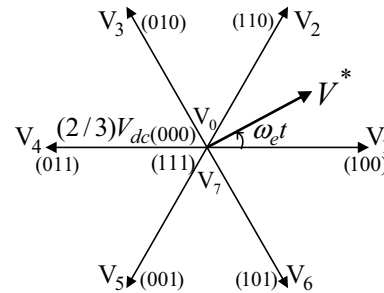


Fig. 3. Voltage space vectors of three-phase two-level inverter. The upper switch states are shown in the brackets ( $S_{a+}$ ,  $S_{b+}$ ,  $S_{c+}$ ). “1” is on and “0” is off state.

## 2. Review of the Carrier-Based PWM Principles

The PWM approach is based on the “per-carrier cycle volt-second balance” principle. According to this principle, in a

PWM period, the average value of the output voltage is equal to the reference value. Thus, an output voltage with a desirable value is obtained by creating a reference voltage and matching this reference voltage with the pulse width modulated inverter output voltages for each pulse period.

In scalar PWM, the reference (modulation) wave is compared with a triangular carrier wave and the intersections define the switching instants. The triangular carrier is used for the symmetric switching sequence which is superior to other sequences due to the low-harmonic-distortion characteristic. The period of the carrier wave is equal to one PWM period ( $T_S$ ). In a PWM period, if the modulation wave is larger (smaller) than carrier wave, the upper switch is on (off). The upper and lower switches of each leg operate in complementary manner ( $S_{a+}=1 \rightarrow S_{a-}=0$ ). The per-carrier cycle average value of the voltage of one VSI leg output is equal to the reference value of that leg due to volt-second balance principle. If a sinusoidal output voltage is wanted, then a modulation wave consisting of sinusoidal form with proper fundamental frequency and magnitude are compared with the high frequency carrier wave.

In a three-phase VSI, the reference (modulation) waves of each leg have the same shape but they are  $120^\circ$  phase shifted from each other. To obtain sinusoidal output voltages, three symmetric and  $120^\circ$  phase shifted modulation waves can be compared with the carrier wave and this method is called as the sinusoidal PWM (SPWM) method and it has been used in motor drives for a long time. However, the inverter performance can be enhanced in three-phase three-wire inverters via signal injection techniques (also additionally using polarity reversing triangle carrier signals) and such techniques have found wide use.

In three-phase three-wire inverter drives (such as motor drives), the neutral point of the load is isolated and no neutral current path exists. The n-o potential in Fig. 1, which will be symbolized with  $v_0$ , can be freely varied. In such applications, any common bias voltage (common mode voltage) can be added (injected) to the reference voltages (modulation waves). If this signal is made to oscillate at a base frequency equal to three times the output voltage frequency ( $\omega_c$ ), it is called the zero-sequence signal. The injection of a zero-sequence signal simultaneously shifts each reference wave in the vertical direction (with respect to the triangular carrier wave). Therefore, the inverter line-to-line voltage per-carrier cycle average value is not affected. But it changes the position of the output line-to-line voltage pulses (Fig. 6). Therefore, it significantly influences the switching frequency characteristics. By injecting different zero-sequence signals, various PWM methods with different characteristics can be generated. The conventional scalar PWM approach with zero-sequence signal injection principle is illustrated in Fig. 4. Note here that only one triangular carrier wave is utilized. In the scalar representation the modulation waves are defined as (1), (2) and (3).

$$v_a^{**} = v_a^* + v_0 = V_{1m}^* \cos(\omega_e t) + v_0 \quad (1)$$

$$v_b^{**} = v_b^* + v_0 = V_{1m}^* \cos(\omega_e t - \frac{2\pi}{3}) + v_0 \quad (2)$$

$$v_c^{**} = v_c^* + v_0 = V_{1m}^* \cos(\omega_e t + \frac{2\pi}{3}) + v_0 \quad (3)$$

where  $v_a^*$ ,  $v_b^*$  and  $v_c^*$  are sinusoidal reference signals and  $v_0$  is the zero-sequence signal. Using the zero-sequence signal injected modulation waves, the duty cycle of each switch can be

easily calculated in the following:

$$d_{x+} = \frac{1}{2} \left( 1 + \frac{v_x^{**}}{V_{dc}/2} \right), \quad \text{for } x \in \{a, b, c\} \quad (4)$$

$$d_{x-} = 1 - d_{x+}, \quad \text{for } x \in \{a, b, c\} \quad (5)$$

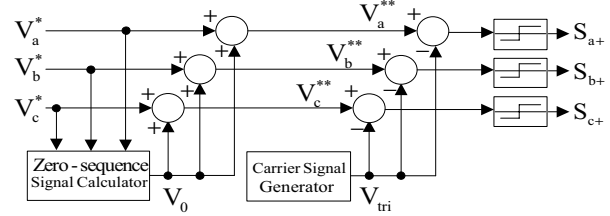


**Fig. 4.** The generalized signal block diagram of the conventional triangle intersection technique-based scalar PWM employing the zero-sequence signal injection principle.

In the space vector approach, employing the complex variable transformation, the time domain modulation signals are translated to the complex reference voltage vector which rotates in the complex coordinates with the  $\omega_e t$  angular speed (Fig. 3) in the following:

$$V^* = \frac{2}{3} (v_a^* + a v_b^* + a^2 v_c^*) = V_{1m}^* e^{j\omega_e t}, \quad \text{where } a = e^{j\left(\frac{2\pi}{3}\right)} \quad (6)$$

Since there are eight possible inverter states available, the vector transformation yields eight voltage vectors as shown in Fig. 3. Of these voltage vectors, six of them ( $V_1, V_2, V_3, V_4, V_5, V_6$ ) are active voltage vectors, and two of them ( $V_0$  and  $V_7$ ) are zero voltage vectors (which provide degree of controllability similar to the zero-sequence signal of the scalar implementation) which generate zero output voltage. In the space vector analysis, the duty cycles of the voltage vectors are calculated according to the vector volt-second balance rule defined in (7) and (8), and these voltage vectors are applied with the calculated duty cycle.

$$V_i t_i + V_j t_j + V_k t_k = V^* T_S \quad (7)$$

$$t_i + t_j + t_k = T_S \quad (8)$$

Each PWM method utilizes different voltage vectors and sequences. Therefore, the vector space is divided into segments. There are 6 A-type and 6 B-type segments available (Fig. 5). Investigations reveal that all PWM methods utilize either A-type or B-type segments, and the utilized voltage vectors of these PWM methods alternate at the boundaries of the corresponding segments [5].

Regardless whether a PWM pulse pattern is implemented with scalar or vector PWM, a given pulse pattern exhibits a specific performance attribute. In the following various methods will be discussed and mainly the scalar implementation will be considered.

### 3. Scalar Implementation of the Carrier-Based PWM Methods

A properly selected zero-sequence signal can extend the volt-second linearity range of conventional SPWM. Furthermore, it

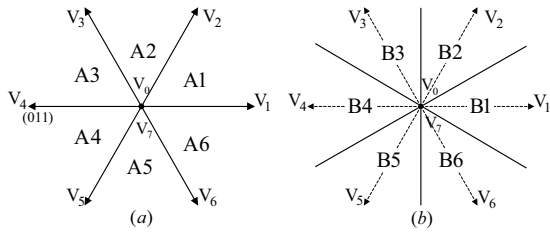


**Fig. 5.** Voltage space vectors and 60° sector definitions: (a) A-type, (b) B-type regions.

can improve the current waveform quality, reduce the switching losses significantly, and/or also reduce the magnitude and rms value of high frequency common mode voltage (CMV) (The CMV of the three-phase VSI is defined as  $v_{cm} = (v_{ao} + v_{bo} + v_{co})/3$ ). Since the VSI can not provide pure sinusoidal voltages and has discrete output voltages, it generates high frequency CMV. Even when no zero-sequence signal is injected (SPWM), the VSI generates high frequency CMV (at the carrier frequency range and much higher) due to discrete output voltages. This causes common mode current (CMC) (leakage current) due to high frequency parasitic components in the drive system and results in performance problems in the application field. It should be noted that the injected zero-sequence signal is a low frequency signal ( $3\omega_c$ ) and causes low frequency CMV. At such frequencies the parasitic circuit components are negligible and therefore the zero-sequence voltage has no detrimental effect on the drive and yields no CMC. High frequency CMV on the other hand can be harmful and can be reduced by PWM pulse pattern modification.

Based on the high frequency CMV property, the PWM methods can be separated into two groups as conventional and reduced CMV PWM (RCMV-PWM) methods. In the conventional PWM methods the CMV takes the values of  $\pm V_{dc}/6$  or  $\pm V_{dc}/2$ , depending on the inverter switch states. The conventional methods utilize zero vectors  $V_0$  and  $V_7$ , and this causes a CMV of  $-V_{dc}/2$  and  $V_{dc}/2$ , respectively. The RCMV-PWM methods, on the other hand, do not utilize zero vectors. Therefore, they limit the CMV to  $\pm V_{dc}/6$ . The most popular conventional methods are SPWM, SVPWM, and DPWM1. Among the RCMV-PWM methods AZSPWM1, AZSPWM3, and NSPWM are the most successful representatives.

Another classification can be made based on the modulation waveform shape, as continuous PWM (CPWM) and discontinuous PWM (DPWM) methods. In the continuous methods, the modulation waves are always within the triangle peak boundaries; within every carrier cycle, the triangle and modulation waves intersect, and on and off switchings always occur. In the discontinuous PWM methods, the modulation wave of a phase has at least one segment which is clamped to the positive or negative dc rail for at most a total of  $120^\circ$ , therefore, within such intervals the corresponding inverter leg is not switched and switching losses are reduced.

SVPWM, AZSPWM1, and AZSPWM3 methods are CPWM methods with the same zero-sequence signal (the same modulation wave). Likewise, DPWM1 and NSPWM are DPWM methods with the same zero-sequence signal and modulation wave. Even though the modulation wave is the same, using different triangular waves makes these PWM methods different and performance characteristics such as CMV, current/voltage ripple and voltage linearity differ.

Although theoretically an infinite number of zero-sequence signals and therefore, modulation methods could be developed, the performance and simplicity constraints of practical PWM-VSI drives reduce the possibility to a small number. Fig. 7 illustrates the modulation and zero-sequence signal waveforms of popular triangle intersection PWM methods. In the figure, unity triangular carrier wave gain is assumed and the signals are normalized to  $V_{dc}/2$ . Therefore, the saturation limits  $\pm V_{dc}/2$  correspond to  $\pm 1$ . In the figure, only the phase “a” modulation wave is shown, and the modulation signals of phases “b” and “c” are identical waveforms with  $120^\circ$  phase shift.

In the scalar PWM implementation, where the reference signal is compared with a triangular carrier signal, there is a linear relation between the reference signal and the output phase voltage. The operation range where this linear relation is satisfied is called voltage linearity region. However this linear relation is violated when the peak value of the reference signal is greater than triangular carrier signal peak value ( $\pm V_{dc}/2$ ). Hence this region is called non-linear (overmodulation) region. In the non-linear overmodulation region, output voltage is always less than the reference value. With the modulation index  $M_i$  ( $M_i = V_{im}/V_{1m6step}$  where  $V_{1m6step} = (2V_{dc}/\pi)$ ) defining the voltage utilization of the inverter, the voltage linearity range of a modulator can be studied. SPWM’s linearity range is  $0 \leq M_i \leq 0.785$ . By injecting a zero-sequence signal linearity range is extended to at most  $M_{i,max} = 0.907$  which is the theoretical linearity limit. The region from  $M_i = 0.907$  to six-step operating point ( $M_i=1$ ) is the overmodulation region. Scalar implementation of the popular high performance PWM methods are described in the following.

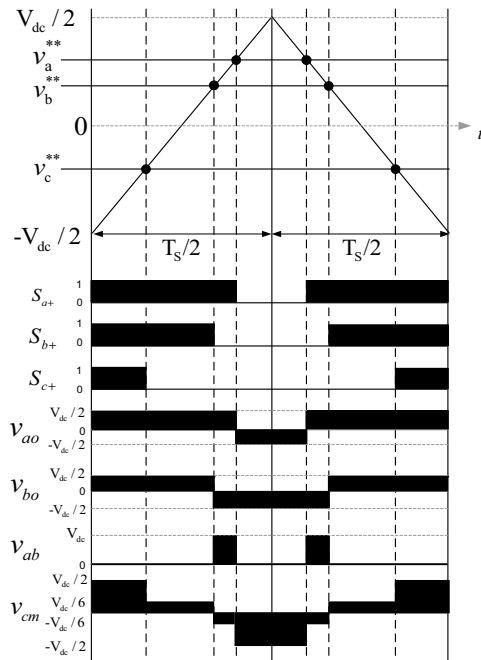


**Fig. 6.** The PWM cycle view of modulation and switch logic signals, phase and line-to-line voltages and CMV of SVPWM.

### 3.1. Conventional PWM Methods

In the conventional methods only one triangular carrier is used. The simplest conventional method is SPWM method. No zero-sequence signal is injected and three-phase sinusoidal reference signals are compared with the same triangular carrier

wave. SPWM's voltage linearity range is limited which ends at  $V_{lm}^* = (V_{dc}/2)$ , i.e., a linearity range of  $0 \leq M_i \leq 0.785$ . And also it has poor waveform quality in the high modulation range. The most popular and high performance conventional methods are SVPWM and DPWM1. Both have linearity range of  $0 \leq M_i \leq 0.907$ . SVPWM has superior output current ripple characteristics. DPWM1 has lower switching loss.

The zero-sequence signal of SVPWM is generated by employing the minimum magnitude test which compares the magnitudes of the three reference signals and selects the signal which has minimum magnitude [1]. Scaling this signal by 0.5, the zero-sequence signal of SVPWM is found. Assume  $|v_a^*| \leq |v_b^*|, |v_c^*|$ , then  $v_0 = 0.5 \cdot v_a^*$ .

In DPWM1, the zero-sequence signal is injected such that reference signal of one phase is always clamped to the positive or negative DC bus. The clamped phase is alternated throughout the fundamental cycle. The phase signal which is the largest in magnitude is clamped to the DC bus with the same polarity [1]. Assume  $|v_a^*| \geq |v_b^*|, |v_c^*|$ , then  $v_0 = (\text{sign}(v_a^*)) \cdot (V_{dc}/2) - v_a^*$ . The modulation waves of SVPWM and DPWM1, which are shown in Fig. 7, can be directly utilized in the following RCMV-PWM methods.

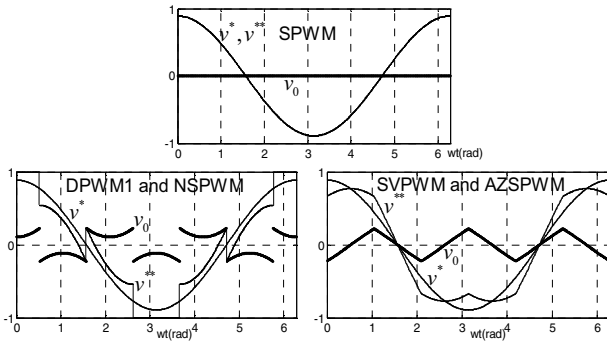


Fig. 7. Modulation waveforms and zero-sequence signals of the modern PWM methods ( $M_i = 0.7$ ).

### 3.2. RCMV-PWM Methods

Among the RCMV-PWM methods, AZSPWM methods and NSPWM provide high performance. Two advantageous AZSPWM methods, AZSPWM1 and AZSPWM3 are discussed. Since they limit CMV to  $\pm V_{dc}/6$ , they have better CMV and CMC characteristics compared to SVPWM. In the AZSPWM methods, instead of the real zero voltage vectors ( $V_0$  and  $V_7$ ) two active opposite voltage vectors with equal time duration are utilized to create effectively a zero vector. The choice and the sequence of the active voltage vectors are the same as in SVPWM. Therefore, in the scalar approach the modulation signals of AZSPWM methods are the same as SVPWM's. However, in AZSPWM methods, instead of one carrier wave, two carrier waves ( $V_{tri}$  and  $-V_{tri}$ ) must be utilized. The implementation of AZSPWM1 and AZSPWM3 is quite easy by using triangular intersection technique. The choice of the triangle to be compared with the modulation signals is voltage vector region dependent and is given in Table 1. All AZSPWM methods have a linearity range of  $0 \leq M_i \leq 0.907$ .

NSPWM, a recently reported DPWM method, has low switching loss and CMV characteristics. But its linearity range is limited to  $0.61 \leq M_i \leq 0.907$ . NSPWM employs only three neighbour active voltage vectors and sequences them in the order that the minimum switching count is obtained. Thus, one of the phases is not switched within each PWM cycle. In the

scalar implementation, the modulation signal of NSPWM and DPWM1 are exactly the same. However, in NSPWM, instead of one carrier wave, two carrier waves ( $V_{tri}$  and  $-V_{tri}$ ) must be utilized. The choice of the triangle to be compared with the modulation signals is region dependent and is given in Table 1.

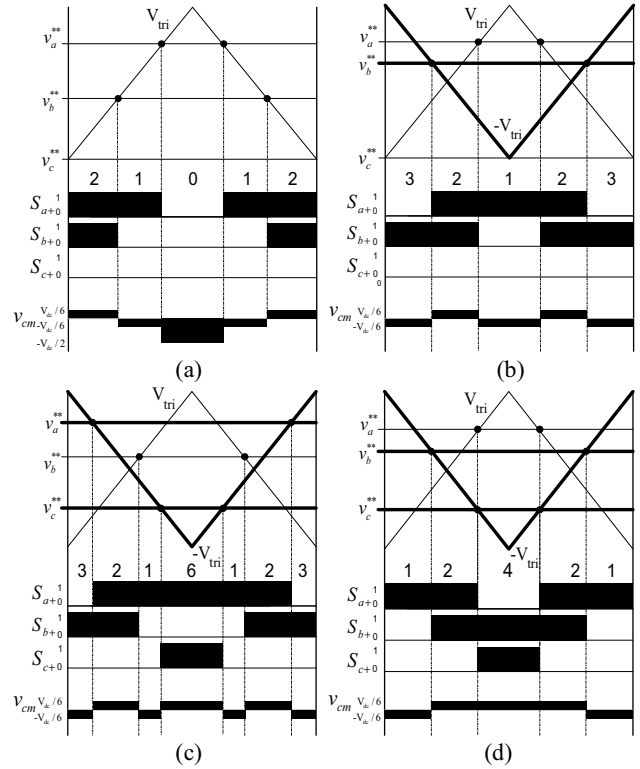


Fig. 8. Pulse patterns of various PWM methods

(a) DPWM1 in region  $A1 \cap B2$ , (b) NSPWM in region B2, (c) AZSPWM1 in region A1, (d) AZSPWM3 in region A1.

Table 1. AZSPWM1, AZSPWM3, and NSPWM space vector region dependent carrier signals

AZSPWM1						
	A1	A2	A3	A4	A5	A6
Phase a	$-V_{m1}$	$-V_{m1}$	$-V_{m1}$	$V_{m1}$	$V_{m1}$	$V_{m1}$
Phase b	$V_{m1}$	$V_{m1}$	$-V_{m1}$	$-V_{m1}$	$-V_{m1}$	$V_{m1}$
Phase c	$-V_{m1}$	$V_{m1}$	$V_{m1}$	$V_{m1}$	$-V_{m1}$	$-V_{m1}$
AZSPWM3						
	A1	A2	A3	A4	A5	A6
Phase a	$V_{m1}$	$V_{m1}$	$-V_{m1}$	$-V_{m1}$	$-V_{m1}$	$V_{m1}$
Phase b	$-V_{m1}$	$V_{m1}$	$V_{m1}$	$V_{m1}$	$-V_{m1}$	$-V_{m1}$
Phase c	$-V_{m1}$	$-V_{m1}$	$-V_{m1}$	$V_{m1}$	$V_{m1}$	$V_{m1}$
NSPWM						
	B1	B2	B3	B4	B5	B6
Phase a	$V_{m1}$	$-V_{m1}$	$-V_{m1}$	$V_{m1}$	$V_{m1}$	$V_{m1}$
Phase b	$V_{m1}$	$V_{m1}$	$V_{m1}$	$-V_{m1}$	$-V_{m1}$	$V_{m1}$
Phase c	$-V_{m1}$	$V_{m1}$	$V_{m1}$	$V_{m1}$	$V_{m1}$	$-V_{m1}$

In the scalar implementation the modulation waves can be generated with a small number of computations (magnitude tests) and PWM methods can be implemented with a microcontroller or DSP. Due to the simplicity of the algorithms, it is easy to program two or more methods and on-line select a modulator in each operating region in order to obtain the highest performance [1]. On the other hand, the vector implementation requires more complex process. First the sector to which the voltage vector belongs has to be identified, then the time length of each active vector must be calculated, and finally gate pulses

must be generated in a correct sequence. Although it is possible to reduce vector implementation PWM algorithms, the effort does not yield as simple and intuitive a solution as the scalar approach [1]. Therefore, scalar PWM implementation is superior to the vector implementation perspective.

#### 4. Experimental Results

Employing the scalar implementation approach and utilizing a digital signal processor with proper PWM signal generator (TMS320F2808), PWM signals are programmed and applied to a three-phase inverter to drive a motor. The resulting modulation waves, phase currents, common mode voltage and currents are shown in Fig. 9 for the considered methods. A 4-kW, 1440  $\text{min}^{-1}$ , 380V<sub>ll-rms</sub> induction motor is driven from a VSI in the constant V/f mode (176.7 V<sub>rms</sub>/50 Hz) and the PWM frequency is 6.6 kHz for CPWM methods and 10 kHz for DPWM methods. Operation at  $M_i=0.8$  (180.3 V<sub>rms</sub>/51 Hz, 1510  $\text{min}^{-1}$ ) is discussed. As can be seen from the diagrams all the discussed methods provide satisfactory performance at the high  $M_i$ . NSPWM provides low motor current ripple and CMV/CMC. SVPWM and DPWM1 have low current ripple but high CMV/CMC. AZSPWM3 has high CMV and CMC magnitude compared to NSPWM, but its CMV/CMC frequency is less. AZSPWM1 has higher PWM current ripple and comparable CMV/CMC to NSPWM.

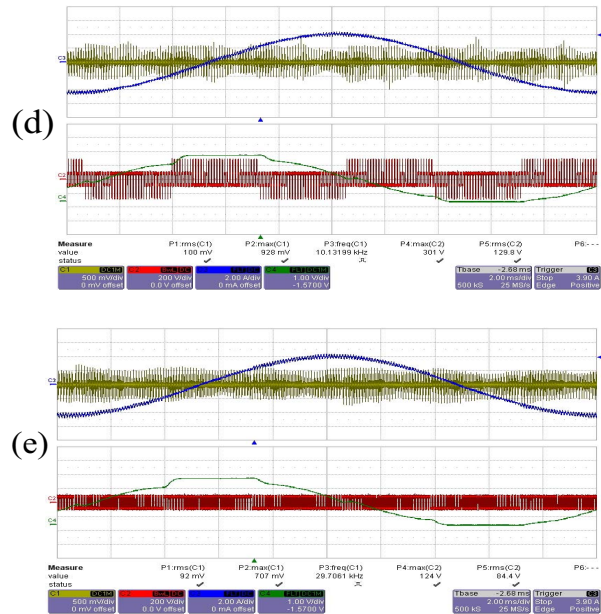
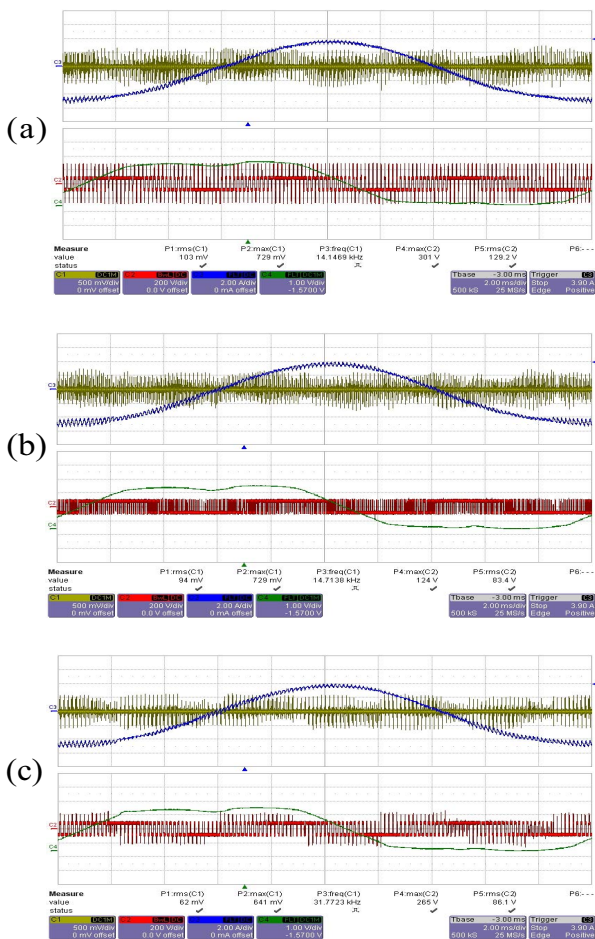


**Fig. 9.** The motor phase current (blue)(2A/div), modulation wave (green)(0.2 unit/div), CMV (red)( 200V/div) and CMC (yellow)(500mA/div) for (a) SVPWM, (b) AZSPWM1, (c) AZSPWM3, (d) DPWM1, (e) NSPWM, (time scale: 2ms/div).

#### 5. Conclusions

PWM principles are reviewed and applied to three-phase inverter drives. Scalar PWM implementation is discussed and applied to the conventional PWM methods and reduced common mode voltage PWM methods. Modulation signal generation and triangle comparison details are provided. It is shown that the scalar approach yields a simple and powerful implementation method. The theory is verified by laboratory experiments. The simple and efficient scalar PWM approach is favorable over the vector PWM approach.

#### 6. References

- [1] A. M. Hava, R. J. Kerkman, and T. A. Lipo, "Simple analytical and graphical methods for carrier-based PWM-VSI drives," *IEEE Trans. Power Electron.*, vol. 14, no. 1, pp. 49–61, Jan. 1999.
- [2] Y.S. Lai, F.S. Shyu, "Optimal common-mode voltage reduction PWM technique for inverter control with consideration of the dead-time effects-part I: basic development," *IEEE Trans. Ind. Applicat.*, vol. 40, pp. 1605-1612. Nov./Dec. 2004.
- [3] E. Ün, A.M. Hava "A near state PWM method with reduced switching frequency and reduced common mode voltage for three-phase voltage source inverters," *IEEE Trans. Ind. Applicat.*, vol. 45, no. 2, pp. 782-793. Mar./Apr. 2009.
- [4] M. Cacciato, A. Consoli, G. Scarcella, A. Testa, "Reduction of Common mode currents in PWM inverter motor drives," *IEEE Trans. Ind. Applicat.*, vol. 35, pp. 469-476. March/April 1999.
- [5] A. M. Hava and E. Ün, "Performance analysis of reduced common mode voltage PWM methods and comparison with standard PWM methods for three-phase voltage source inverters," *IEEE Trans. Power Electron.*, vol. 24, no. 1, pp. 241–252, Jan. 2009.